The Scientific Journal of University of Benghazi

www.sjuob.uob.edu.ly

Geochemical Characterization Of the U1 Member, Sahabi formation In Northeast Sirt Basin, Libya

Osama R. Shaltami [1], Ahmed M. Muftah [1*], Moftah, H. El-Shawaihdi [1], Osama A. El-Fallah [1]

[1] *University of Benghazi, Faculty of Science, Department of Earth Sciences, Benghazi-Libya.*

Received: 07 / 07 / 2020; Accepted: 31 / 12 / 2020

الملخص:

هذه الورقة اعتمدت على دراسة جيوكيميائية عينات صخور طينية أخذت من ثلاثة مكاشف لعضو U1 من تكوين الصحابي في منطقة الصحابي شمال شرق حوض سرت. يعتبر هذا العضو الطبقة الأكثر احتواءً على بقايا مستحاثات الأسماك والزواحف والثدييات. بعض العينات التي جُمِعَتْ أجري لها تحليل جيوكيميائي باستخدام جهاز Perkin Elmer the ICP-OES)) لمعرفة الأكاسيد السائدة وتحليل جيوكيميائي آخر باستخدام جهاز (Perkin Elmer SciexElan 9000 ICP-MS) لمعرفة العناصر النادرة. استُخْدِمت برامج إحصائية لتحديد نسب العناصر المعنية للتعرف على المصدر والبيئة الترسيبية والتعرية القديمة والمناخ القديم والوضع التكتوني للعينات المدروسة في هذا العضو الطيني.

الكلمات المفتاحية:

جيوكيمياء، طين، بيئة ترسيبية، تكوين الصحابي، حوض سرت، ليبيا.

Abstract

This study is based on three cropped out clay profiles belonging to U1 Member of the Sahabi Formation at As Sahabi area in northeast Sirt Basin. This member horizon is the most productive layer in terms of fish, reptiles and mammals remains. Some of the collected samples were subjected to geochemical analysis using Perkin Elmer the ICP-OES to define the major oxides and Perkin Elmer SciexElan 9000 ICP-MS for trace elements. The statistical relationships between relevant elemental percentages have been used to determine the provenance, depositional environment, paleo-weathering, paleo-climate and tectonic setting.

Keywords: Geochemistry, Clay, Depositional Environment, Sahabi Formation, Sirt Basin, Libya.

1. INTRODUCTION

The present study is a detailed geochemical investigation of the clayey portion of Member U1 of the Sahabi Formation. The As Sahabi area is located in the Ajdabiya Trough of Northeast Sirt Basin, with an area covering approximately 375km^2 and bounded by longitudes 20º 48' 08" to 20º 54' 45" E and latitudes 30º 10' 58" to 30º 17' 36" N (Fig. 1).

The studied profiles P96c, P25, P28 are located precisely at (30º 12' 1.15" N & 20º 50' 35.15" E), (30º 13' 47.12" N 20º 51' 18.52" E), (30º 13' 56.69" N 20º 51' 26.71" E), respectively (Figs. 2,3 and 4).

The aim of this work is to determine the elemental percentages of the studied clays from Member U1 of Sahabi Formation. These geochemical data will be statistically analyzed to interpret the depositional environment, paleoweathering, paleoclimate, tectonic setting and provenance.

Very rare geochemical studies have been conducted in As Sahabi area, however, regarding the presence of different types of clays (common smectite with minor kaolinite) as mentioned in[2], stratigraphical surveying of the As Sahabi area. De Geyter and Stoops, (1987) have also mentioned the presence of Montmorillonite, Kaolinite and weathered mica in variable proportions[3].

The Precambrian continental rocks in NE Chad were suggested to be the source of Member U1clays by[1], as well as[4], based on the mineralogical and geochemical analysis of Member U1 of Sahabi Formation from same localities used in this work. Muftah and El Ebaidi, published a mineralogical and geochemical analysis investigations of the Neogene members (U1 and U2) of the Sahabi Formation in Northeast Sirt Basin[5].

Methodology

This study is based on a total of eight selected samples collected from three outcrops in As Sahabi area (Fig. 1) during 2010 field season of the East Libya Neogene Research Project (ELNRP). Six samples were collected

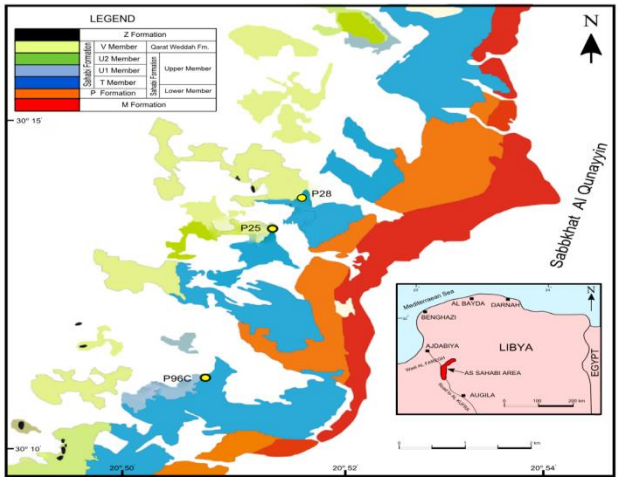


Figure 1. Geological Map shows locations of the three sampled profiles at the As Sahabi area.

from Profile 25 (P25) (Fig. 2), one sample from Profile 28 (P28) (Fig, 3) and another one sample from Profile (P96c) (Fig. 4), all are from Member U1 of the Sahabi Formation. Perkirn Elmer

*Correspondence:

Ahmed M. Muftah

ahmed.alkowafi@uob.edu.ly

the ICP-OES was used to analyze the major oxides, while the trace elements were analyzed by Perkin Elmer SciexElan 9000 ICP-MS. The analytical procedure depends on the decomposition of exact weight of 0.2 g powdered fine sand size sample in 50 ml Teflon beaker. Decomposition was done by 4 ml HNO3, 3 ml HClO4 and 5 ml HF, and evaporated to dryness under 200oC. The residue was dissolved with 5 ml (1:1) HNO3 by heating and 5 ml of 4 ppm indium solution was added as an internal standard. The sample, as well as standard, solutions were introduced by peristaltic pump with 0.18.

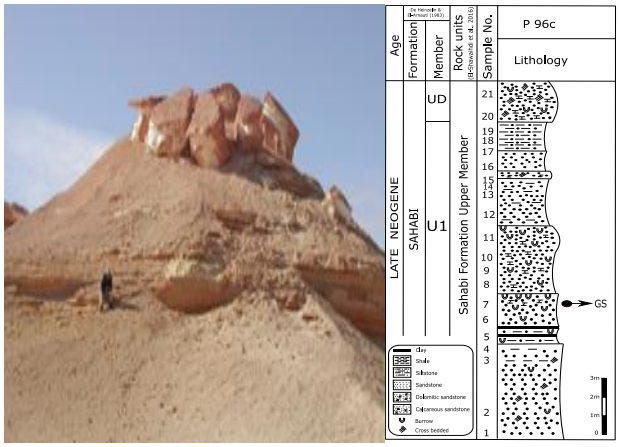


Figure 2. Close view and stratigraphic column of the sampled new profiles P96c (modified after[1]). (the geochemical analysed sample indicated by arrow)

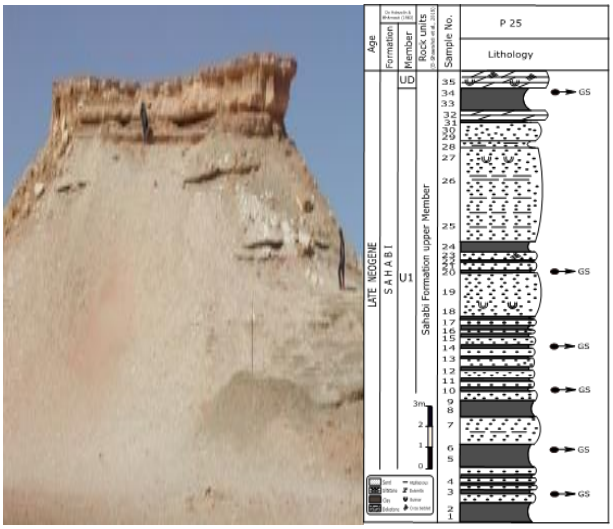


Figure 3. Close view and stratigraphic column of the sampled monkey hill profiles P25 (modified after[1]).(the geochemical analysed sample indicated by arrow)

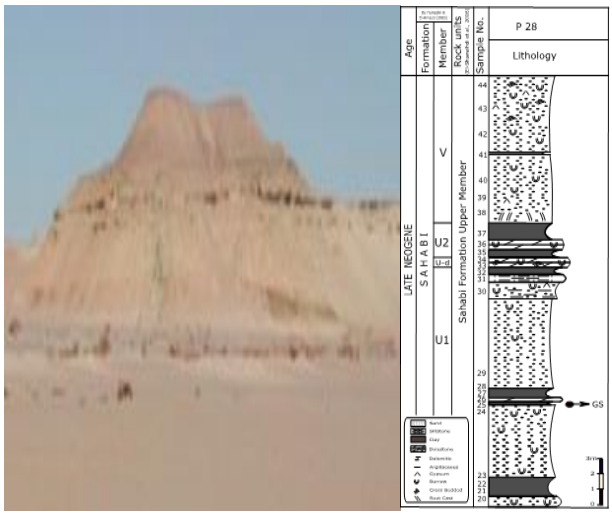


Figure 4. Close view and stratigraphic column of the sampled elephant hill profiles P28 (modified after1. (the geochemical analysed sample GS indicated by arrow).

2. STRATIGRAPHY:

The exposed sections at As Sahabi area are mainly of Neogene age and were studied by [2,6], [7] [8], [1], [9] and [10]. The later stratigraphical study are followed herein, where the four formations, from oldest to youngest (Fig. 5):

1. M Formation: Semi consolidated bioclasts exposed in floor of the Sebkhat, totally or partially decalcified and gypsified. Erosional relief of shallow reefs "MR" with corals, echinoids, pelecypodsand gastropods [10].
2. Sahabi Formation: It can be subdivided into two members: i) the lower member, which is semi-consolidated sandy, gypsiferous and dolomitic limestone with selenite filled fractures (~5 m deep) at upper part. ii) the upper member containing member- U1 which containing fish teeth, reptilians and land mammals.
3. Qarat Weddah Formation (≈ Member "V" of Sahabi Formation[2]) which made of sands and sandy clays with local lenses of dolomite and gypsum crystals in places, however, this formation at Al Jaghbub area was suggested to be up-ranked as a group level by [11].
4. Z Formation is representing a very complex fossil soil capping Qarat Weddah Formation (≈ Member "V" of Sahabi Formation[2]).

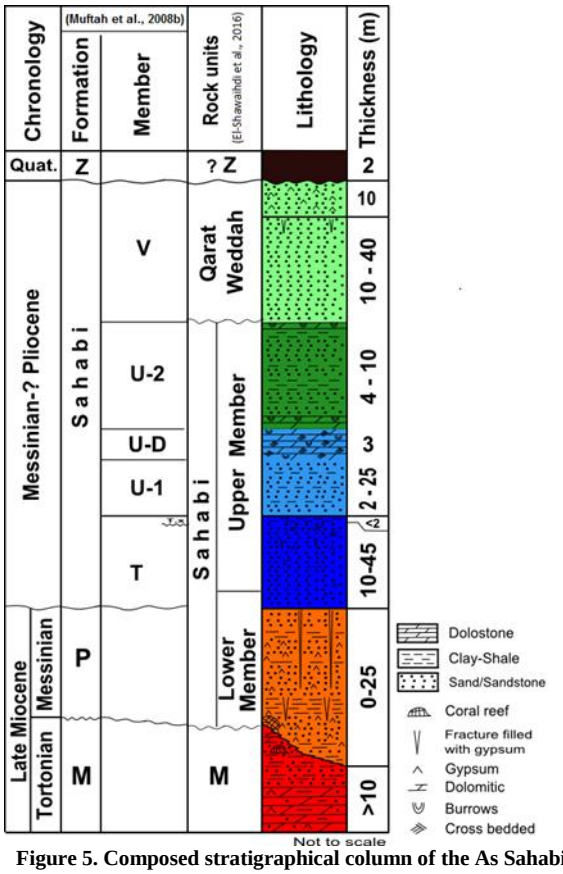


Figure 5. Composed stratigraphical column of the As Sahabi area (modified after [6]).

3. RESULTS AND DISCUSSIONS:

1. Normalization to Post-Archean Australian Shale (PAAS)

The chemical analysis data of the studied samples are shown in Tables (1 and 2). The studied samples contain high concentrations of some major oxides such as SiO2 (52.22-74.68%), Al2O3 (3.35-17.13%), Fe2O3 (1.48-7%), Na2O (0.91-5.52%) and K2O (1.04-2.59%). Moreover, there are also high concentrations of some trace elements such as Rb (29.3-87ppm), Ba (170-261ppm) and Zr (138.9-325.5ppm). The chemical composition of the studied samples is normalized to data of the Post-Archean

Australian Shale (PAAS) as quoted by12. The normalized data (Fig. 6) suggest the following inferences:

- The studied samples show depletions in most major oxides and trace elements.
- There are notable enrichments in Na2O, Nb and U in most samples.
- All samples contain low CaO content for sample P96c, where the sands are the dominant component of the lithology.

SiO2 and Al2O3 are negatively correlated (r = -0.94, Fig. 7), where high SiO2 (52.22- 74.68%) congregates variable Al2O3 (3.35-17.13%). However, there is less SiO2 except P96c locality where there is excess SiO2 (mostly due to quartz) but less Al2O3. It is evident that the intimate coherence between Al2O3 and K2O (r = 0.96) is dependent on the illitic nature. This assumption is further supported by the K2O/Al2O3 ratio (0.15-0.31) and the ternary plot of A-CN-K (Al2O3-(CaO*+Na2O)-K2O) (Fig. 8). CaO correlates moderately with MgO (r = 0.67, Fig. 9). This relationship means that dolomite is not the sole carrier of MgO.

Table 1. Chemical analysis data (major oxides in wt. %) of the studied samples

Oxides	Sample No.							
	P25-34	P25-20	P25-15	P25-10	P25-6	P25-3	P28-25	P96c
SiO_2	54.80	66.31	53.20	54.35	65.18	52.22	67.20	74.68
TiO_2	0.70	0.55	1.03	1.14	0.77	1.05	0.70	0.16
Al_2O_3	14.34	8.36	15.87	17.13	11.56	17.12	12.03	3.35
Fe_2O_3	7.00	4.35	5.23	5.02	5.58	6.76	4.31	1.48
MnO	0.02	0.01	0.02	0.02	0.03	0.02	0.02	0.05
MgO	2.98	1.36	2.29	2.48	1.79	2.20	2.13	3.43
CaO	0.12	0.18	0.24	0.29	0.27	0.33	0.67	5.10
Na_2O	3.61	5.52	3.95	2.94	3.08	3.22	0.91	0.94
K_2O	2.31	1.35	2.34	2.49	2.03	2.59	2.30	1.04
P_2O_5	0.05	0.08	0.06	0.06	0.11	0.08	0.04	0.06
LOI	13.90	11.80	15.60	13.90	9.40	14.20	9.60	9.60

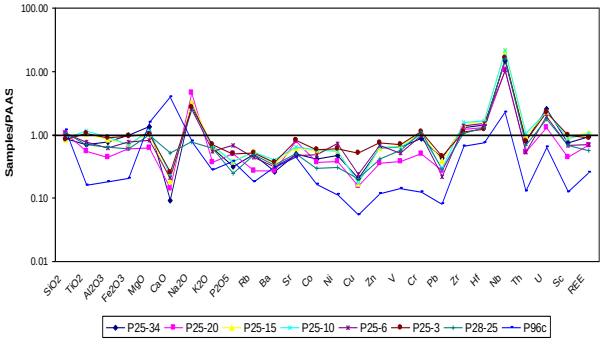


Figure 6. Major oxides and selected trace elements content of the studied samples normalized to the data of the Post-Archean Australian Shale (PAAS) [12]

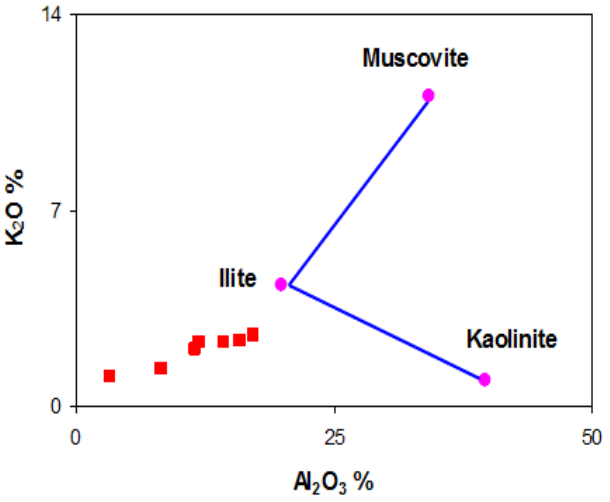


Figure 7. Binary plot of Al2O3 vs. K2O showing the clay minerals in the studied samples (fields after13)

Table 2. Chemical analysis data (trace elements in ppm) of the studied samples

Elements	Sample No.							
	P25-34	P25-20	P25-15	P25-10	P25-6	P25-3	P28-25	P96c
Rb	77.00	42.70	87.00	83.90	70.40	81.40	78.40	29.30
Cs	4.10	1.90	3.20	4.20	4.20	4.70	3.70	1.00
Ba	170.00	175.00	229.00	261.00	202.00	236.00	216.00	201.00
Sr	98.90	161.00	123.20	126.60	94.40	165.90	99.80	88.00
Be	4.00	2.00	2.00	3.00	2.00	3.00	1.00	<1.00
Co	9.70	8.50	12.50	13.50	11.10	13.50	6.90	3.80
Ni	26.00	21.00	30.90	30.00	40.40	33.50	16.70	6.30
Cu	10.20	7.80	8.60	8.70	11.90	25.50	10.20	2.70
Zn	53.00	30.00	52.00	55.00	58.00	63.00	35.00	10.00
V	96.00	56.00	101.00	95.00	78.00	106.00	86.00	21.00
Cr	95.20	54.40	115.60	108.80	108.80	122.40	122.40	13.60
Mo	6.40	1.30	0.10	< 0.10	1.30	0.20	0.20	1.80
Pb	8.70	5.40	7.80	6.00	4.30	9.20	5.70	1.60
As	4.00	7.80	1.10	< 0.50	6.80	1.70	1.60	2.60
Se	< 0.50	< 0.50	0.09	< 0.50	< 0.50	< 0.50	0.09	< 0.50
Sb	< 0.10	< 0.10	0.10	< 0.10	< 0.10	< 0.10	0.10	0.20
Sn	3.00	1.00	4.00	4.00	2.00	4.00	3.00	<1.00
Cd	< 0.10	< 0.10	0.09	< 0.10	< 0.10	< 0.10	0.09	< 0.10
Ga	19.00	11.60	22.70	22.70	14.90	23.50	16.90	4.20
Tl	0.10	< 0.10	0.10	0.10	0.10	0.10	0.30	< 0.10
Hg	< 0.01	< 0.01	0.01	< 0.01	< 0.01	< 0.01	0.01	< 0.01
Bi	< 0.10	< 0.10	0.10	< 0.10	< 0.10	< 0.10	0.10	< 0.10
W	1.60	1.10	2.10	1.90	1.10	2.20	1.40	< 0.50
Zr	272.70	259.30	302.00	325.50	286.00	236.10	223.30	138.90
Hf	7.20	6.40	8.20	8.40	7.50	6.20	6.50	3.70
Nb	28.30	19.90	41.30	40.90	20.20	30.40	29.70	4.30
Ta	1.90	1.30	2.60	2.90	1.50	2.10	1.90	0.30
Th	11.60	7.70	14.10	15.40	7.80	11.70	9.90	1.90
U	8.00	4.00	7.10	7.30	6.00	7.10	5.50	2.00
Sc	12.00	7.00	15.00	14.00	11.00	16.00	11.00	2.00
Y	18.40	14.70	23.90	28.80	18.90	20.00	13.80	7.70
La	44.20	32.00	46.50	44.50	27.70	40.10	24.20	8.70
Ce	69.30	52.50	75.50	73.40	53.70	62.20	37.70	19.50
Pr	8.78	5.76	10.53	9.85	6.37	8.41	5.51	2.21
Nd	30.00	20.80	42.70	38.60	23.50	32.80	21.70	8.40
Sm	5.61	3.67	6.92	7.73	4.60	5.89	3.37	1.79
Eu	1.04	0.74	1.32	1.51	1.02	1.17	0.67	0.46
Gd	4.51	3.19	5.32	6.47	4.02	4.71	2.81	1.51
Tb	0.69	0.52	0.87	1.03	0.65	0.74	0.50	0.27
Dy	3.46	2.90	4.71	5.26	3.35	4.02	2.56	1.42
Ho	0.76	0.60	0.89	1.12	0.70	0.78	0.47	0.31
Er	2.16	1.72	2.51	3.18	2.07	2.14	1.45	0.82
Tm	0.34	0.25	0.39	0.46	0.31	0.35	0.22	0.12
Yb	2.21	1.83	2.60	2.94	2.10	2.17	1.52	0.89
Lu	0.33	0.26	0.40	0.45	0.28	0.34	0.24	0.10

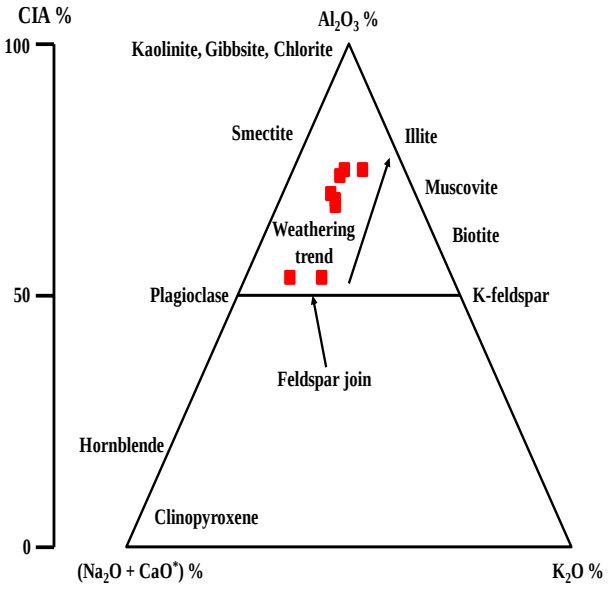


Figure 8. A-CN-K ternary diagram showing the clay minerals in the studied samples (fields after [14])

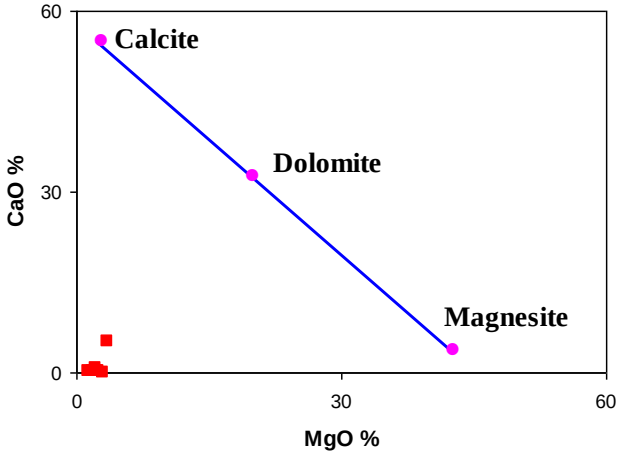


Figure 9. Binary plot of MgO vs. CaO showing the carbonate minerals in the studied samples (fields after [13]).

2. Provenance

Based on the geochemical composition [15] divided the provenance components into five types, namely old upper continental crust (OUC), recycled sedimentary rocks (RSR), young undifferentiated arc (YUA), young differentiated arc (YDA) and exotic components. The studied samples show low Th/U ratio (0.95-2.11),high Th/Sc ratio (0.71-1.1) and positive Eu anomaly (0.97-1.32), suggesting young undifferentiated arc (YUA) (Table 3). It should be noted that the analyzed REE are normalized to Post-Archean Australian Shale (PAAS) as quoted by [12].

Table 3. Geochemical characteristics of sediment derived from different provenance types (after [15])

Provenance type	Eu/Eu*	Th/Sc	Th/U	Others
Old upper continental crust	0.6-1.1	1.0	>3.8	Evolved major element composition (e.g. high Si/Al, CIA) high LILE abundance, uniform compositions
Recycled sedimentary rocks	0.6-1.1	≥ 1.0	>3.8	Evidence of heavyminerals concentration from trace elements (e.g. Zr,Hf for zircon)
Young differentiated arc	0.5-0.9	1.0 to <0.01	<3.0	Evolved major element composition (e.g. high Si/Al, CIA) high LILE abundance variable compositions
Young undifferentiated arc	1.0	1.0 to <0.01	<3.0	Unevolved major element composition (e.g. low Si/Al, CIA) low LILE abundance variable compositions

Several ratios can be used to determine the provenance of sediments such as La/Sc, Th/Sc and Th/Co (Table 4, [16]) These ratios suggest that felsic rocks may be the probable source for the studied sediments. This assumption is also supported by the binary plots of Zr versus TiO2 (Fig. 10), Ni versus TiO2 (Fig. 11), Hf versus La/Th (Fig. 12), and La/Sc versus Th/Co (Fig. 13), and the ternary plot of SiO2/10-CaO*+MgO-Na2O+Ka2O (Fig. 14).We believe that the possible source of the studied sediments is the Precambrian granites of northeastern Chad, as suggested previously by [4].

Table 4. Elemental ratios of the studied samples compared to the ratios derived from felsic rocks, mafic rocks (after [16]) and Post-Archean Australian shale (after [12])

Ratio	Mafic rocks	Felsic rocks	PAAS	Present study
La/Sc	0.43 - 0.86	2.5 - 16.3	2.4	2.2 - 4.57
Th/Sc	0.05 - 0.22	0.84 - 20.5	0.9	0.71 - 1.1
Th/Co	0.04 - 0.4	0.67 - 19.4	0.63	0.5 -1.43

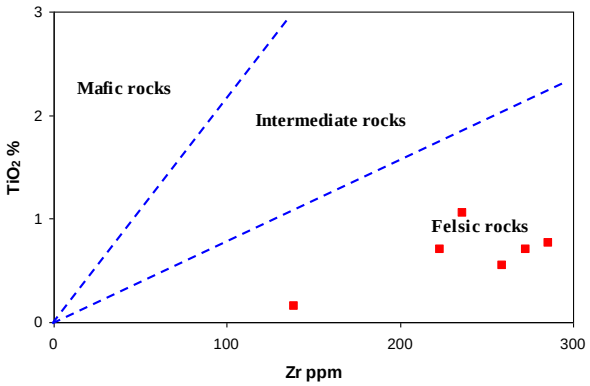


Figure 10. Binary plot of Zr vs. TiO2 showing the provenance of the studied sediments (fields after [17]).

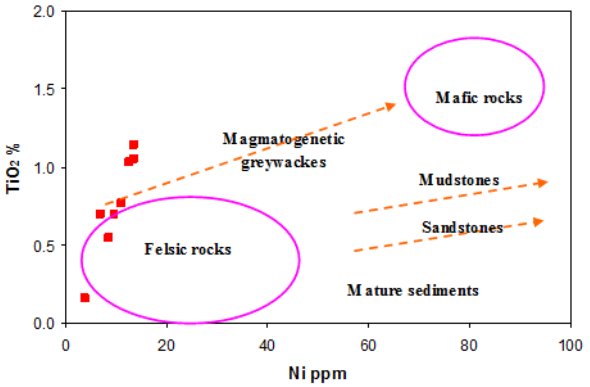


Figure 11. Binary plot of Ni vs. TiO2 showing the provenance of the studied sediments (fields after [18]).

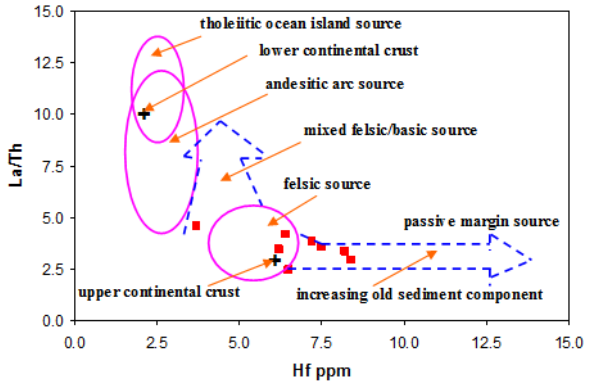


Figure 12. Binary plot of Hf vs. La/Th showing the provenance of the studied sediments (fields after [19]).

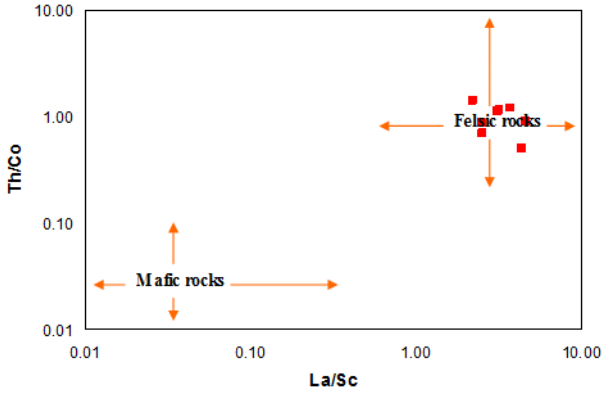


Figure 13. Binary plot of La/Sc vs. Th/Co showing the provenance of the studied sediments (fields after [16]).

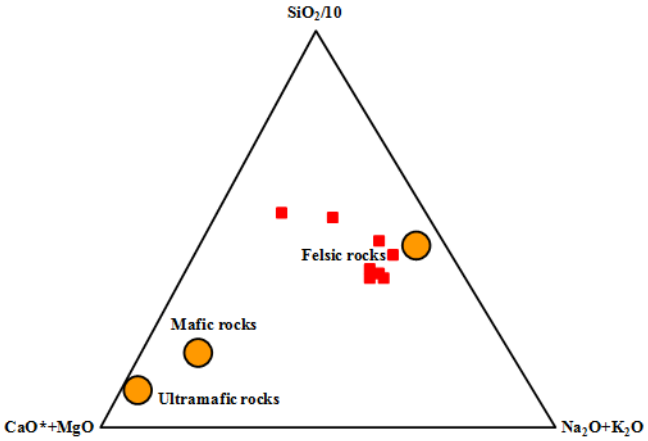
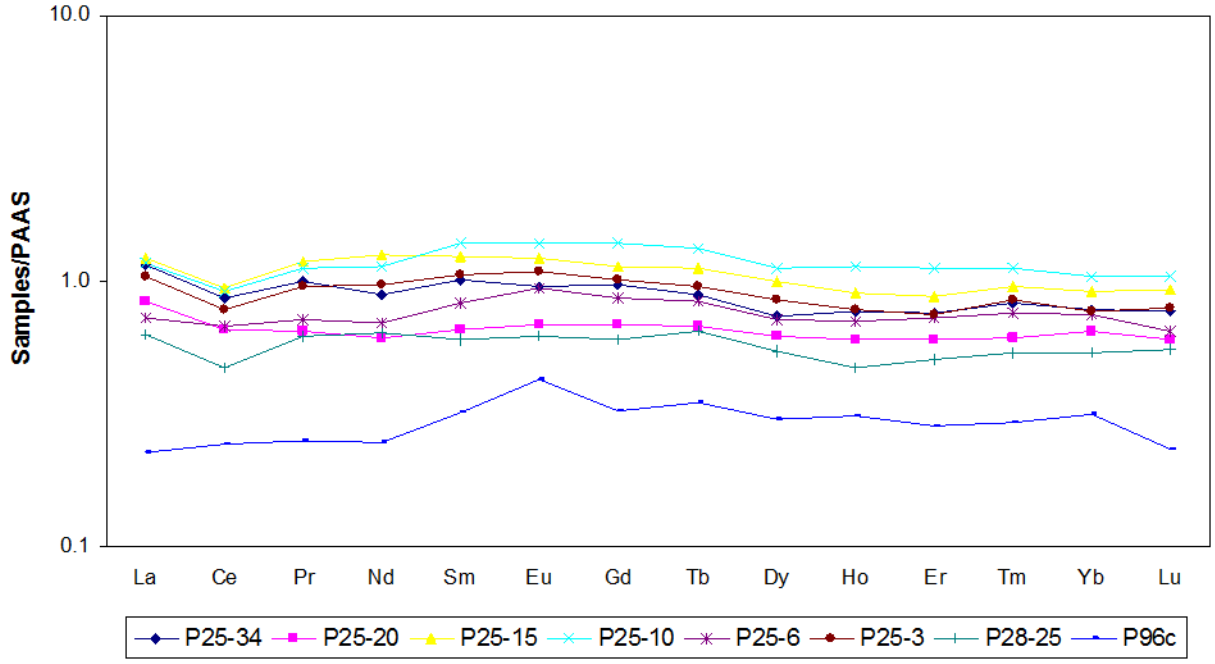


Figure 14. Ternary plot of SiO2/10-CaO*+MgO-Na2O+Ka2O showing the provenance of the studied sediments (CaO* is the content of CaO incorporated in silicate fraction, fields after [12]).

3. Depositional Environment

Figure (15) shows the PAAS-normalized REE patterns of the studied sediments. The samples show flat REE pattern with negative and positive Ce anomalies (0.75-1), and positive Eu anomalies (0.97-1.32), suggesting deposition in a marine environment. The binary plot of (La/Sm)N versus (La/Yb)N (Fig. 16) supports this assumption. There is a clear terrestrial contamination in the sediments. The low Er/Nd ratio (0.06-0.1) and the binary plot of Nb/U versus (La/Sm)N (Fig. 17) also indicating a continental contamination. Furthermore, the Sr/Ba ratio (0.44-0.92)indicate high salinity during deposition.



Figore 15. PAAS normalized REE diagram for the studied sediments.

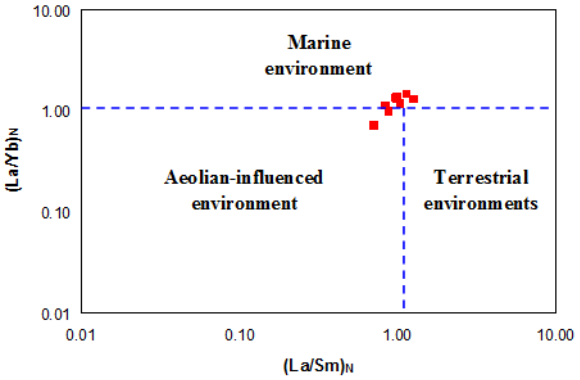


Figure 16. Binary plot of (La/Sm)N vs. (La/Yb)N showing the depositional environment of the studied sediments (fields after [20]).

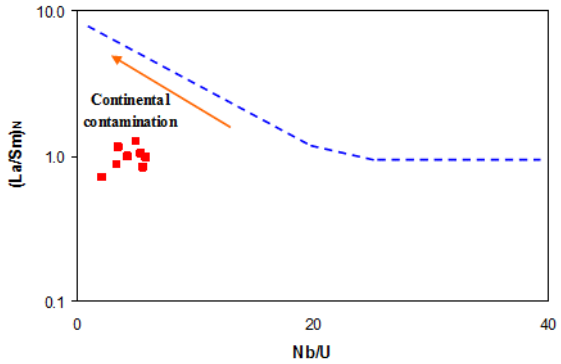


Figure 17. Binary plot of Nb/U vs. (La/Sm)N showing the continental contamination in the studied sediments (fields after [21]).

To define the redox condition, several ratios such as Ni/Co, Cu, Zn, V/Cr and U/Th as well as authigenic uranium (AU = U-(Th/3) were used. In anoxic conditions, these parameters are high, whereas low values point to oxic conditions (Table 5).The studied samples show low values of the redox parameters (Table 5), suggesting deposition in oxic conditions.

Table 5. Redox classification using trace element ratios (after [22], [23], [24] and [25])

Parameter	Oxic conditions	Anoxic conditions	Present study
Ni/Co	<5	>5	1.66 - 3.64
Cu/Zn	<2	>2	0.16 - 0.4
V/Cr	<2	>2	0.7 - 1.54
U/Th	<1.25	>1.25	0.47 - 1.05
AU	<5	>5	1.37 - 4.13

4. Paleoweathering

There are many indices of chemical weathering such as chemical index of alteration (CIA), chemical index of weathering (CIW), plagioclase index of alteration (PIA) and a modified version of CIW (CIW´) ([14], [26], [27] and [28]. The equations of the these indices are:

$$CIA = (Al_2O_3/(Al_2O_3+CaO^*+Na_2O+K_2O))100$$

$$PIA = ((Al_2O_3-K_2O)/((Al_2O_3-K_2O)+CaO^*+Na_2O))100$$

$$CIW = (Al_2O_3/(Al_2O_3+CaO^*+Na_2O))100$$

$$CIW' = (Al_2O_3/(Al_2O_3+Na_2O))100$$

In the studied samples, the degrees of CIA, CIW, PIA and CIW´ vary from 53.43 to 75.8, 55.13 to 86.34, 59.8 to 88.65 and 60.23 to 92.97, respectively, suggesting moderate to high degree of chemical weathering.

5. Paleoclimate

According to [29], the increasing value of the Sr/Cu ratio (>5) suggests a hot-arid climate whereas decreasing Sr/Cu values indicate a warm-humid climate. The Sr/Cu ratio is very high (6.51-32.59) in the studied samples, indicating a hot-arid climate. But the binary plot of(Al2O3+K2O+Na2O) versus SiO2 (Fig. 18) refutes the assumption mentioned above.

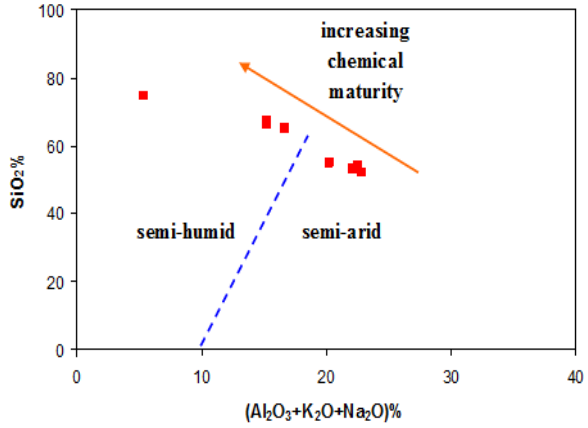


Figure 18: Binary plot of (Al2O3+K2O+Na2O) vs. SiO2 showing the paleoclimate conditions for the studied sediments (fields after [30]).

6. Tectonic Setting

The tectonic settings include oceanic island arc (A), continental island arc (B), active continental margin (C) and passive continental margin (D) (e.g., [31]).To evaluate the tectonic setting of the studied sediments we used three models: the binary plots of Al2O3/(100-SiO2) versus Fe2O3/(100-SiO2) (Fig. 19)and Sc versus V (Fig. 20), and the ternary plot of Hf/3-Th-Nb/16 (Fig. 21). These models show that the continental margin (C and D) is the main tectonic setting.

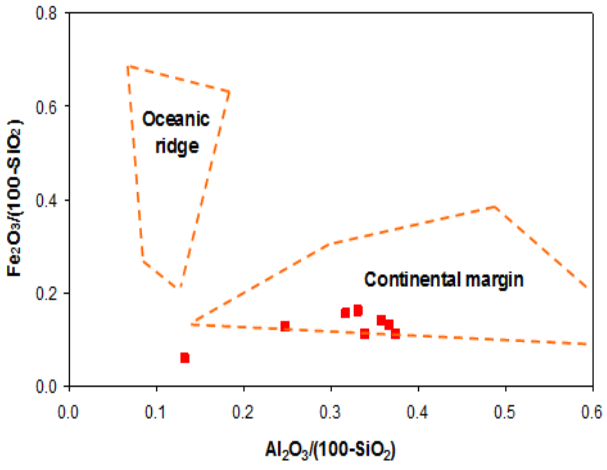


Figure 19: Binary plot of Al2O3/(100-SiO2) vs. Fe2O3/(100-SiO2) showing the paleotectonic setting for the studied sediments (fields after [32]).

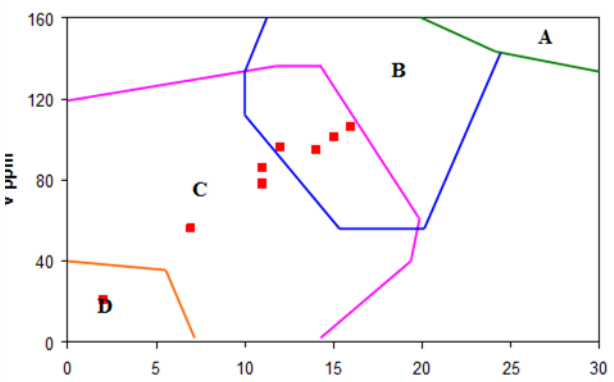


Figure 20: Binary plot of Sc vs. V showing the paleotectonic setting for the studied sediments (fields after [33]).

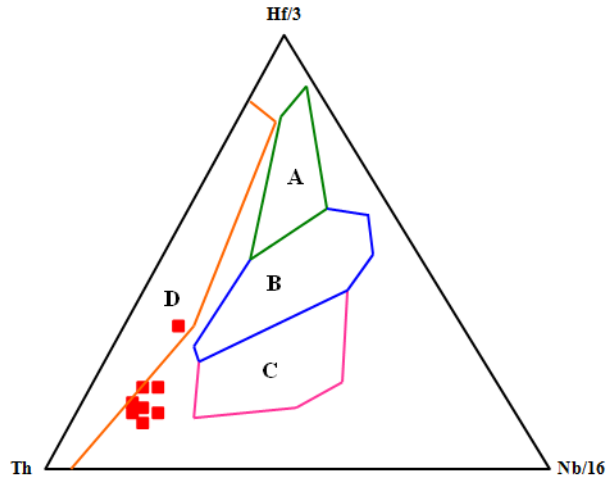


Figure 21: Ternary plot of Hf/3-Th-Nb/16 showing the paleotectonic setting for the studied sediments (fields after [34]).

4. CONCLUSIONS

This study concluded that, the main clay mineral in the clayey portion of Member U1 (i.e. middle clay of the Upper Member) of the Sahabi Formation is illite. The studied clay was deposited in a marine environment under an oxic conditions. with a clear continental contamination. The paleotectonic setting of the studied clay is the continental margin were prevalent during deposition. There was a fluctuation in paleoclimate between semi-humid to semi-arid. The degree of chemical weathering in the source area ranged between moderate to high. The Precambrian granites of northeastern Chad is the possible source of the studied clay.

5. ACKNOWLEDGEMENTS

The authors would like to thank all members of the East Libyan Neogene Research Project (ELNRP from for their support and accompany during field and laboratory works. Dr. A. Godelitsas from University of Athens is highly appreciated for the valuable advice in study.

6. REFERENCES

1. Muftah AM. Biostratigraphic and temporal relations between the Neogene Sahabi and Marada Formations, Libya). Contribution to the age determination of their contained mammalian paleofaunas. Unpublished PhD Thesis, University of Athens, Greece. 2013.

2. De Heinzelin J, El-Arnauti A, editor. Geology of the Sahabi area with a geological map at scale 1:25000. Research Centre of Garyounis University, Benghazi, Libya. (Edited by the section of Cartography and Photo-Interpretation of the Royal Museum for Central Africa, Tervren, Belgium) in commission of the Research Centre, Caryounis University, Benghazi, Libya; 1983.

3. De Geyter G, Stoops G. Petrography of Neogene Sediments of the Sahabi Area: A preliminary report. In: (eds. Boaz, N., El-Arnauti, A., Gaziry, A., De Heinzelin J., Boaz, D.D.) Neogene Paleontology and Geology of Sahabi. Alan R. Liss, New York; 1987. p. 23-36.

4. Muftah AM., Pavlakis P, Godelitsas A, Gamaletsos P, Boaz, NT. Paleogeography of the Eosahabi River in Libya: New Insights into the Mineralogy, Geochemistry and Paleontology of Member U1 of the Sahabi Formation, Northeastern Libya. Journal of African Earth Sciences; 2013. 78: p. 96-86.

5. Muftah AM, El Ebaidi SK. Mineralogical and geochemical investigations of the Upper Neogene Sahabi clays in As Sahabi area-Northeast Sirt Basin. In: The 12th Mediterranean Petroleum conference and Exhibition, Tripoli, Libya; 2012. p. 198-191.

6. De Heinzelin J. El-Arnauti A. The Sahabi Formation and related deposits. In: Boaz N, El-Arnauti A, Gaziry A, De Heinzelin J, Boaz, DD, editors. Neogene Paleontology and Geology of Sahabi. Alan R. Liss, New York; 1987. p. 21-1.

7. Muftah AM, Salloum F, El-Shawaihdi MH, Al-Faitouri MS. A. contribution to the stratigraphy of Formations of the As Sahabi Area, Sirt Basin, Libya. In: Boaz, NT., El-Arnauti A, Pavlakis P, Salem MJ, editors. Garyounis Scientific Bulletin, Special Issue; 5: 2008a. p. 33-45.

8. Muftah AM, El Mehaghag AA, Starkie S, Biostratigraphical notes on the As Sahabi stratigraphic boreholes 1 and 2, Sirt Basin, Libya. In: Boaz NT, El-Arnauti A, Pavlakis P, Salem M J. editors. Garyounis Scientific Bulletin, Special Issue; 5. 2008b. p. 47-57.

9. El-Shawaihdi MH, Muftah, AM, Mozley, PS, Boaz, NT. New age constraints for Neogene sediments of the Sahabi area, Libya (Sirt Basin) using strontium isotope (87Sr/86Sr) geochronology and calcareous nannofossils. Journal of African Earth Science; 89; 2014. p. 42-29.

10. El-Shawaihdi MH, Mozley PS, Boaz NT, Salloum F, Pavlakis P., Muftah AM, Triantaphyllou, M, Stratigraphy of the Neogene Sahabi units in the Sirt Basin, northeast Libya. Journal of African Earth Sciences; 118; 2016. p. 106-87.

11. Shaltami, O.R., Fares, F.F., EL Oshebi, F.M., Errishi, H., Bustany, I. and Musa, M.M. (2018): Depositional environment and absolute age of the Pliocene-Early Pleistocene sediments in the Cyrenaica Basin, NE Libya. 16th Annual Conference on Isotope Geology (ACIG-16), Department of Geosciences and Natural Resource Management, Faculty of Science, University of Copenhagen, Denmark, Proceeding Book; pp. 67-83.

12. Taylor, S.R. and McLennan, S.M. The Continental Crust: Its Composition and Evolution. Blackwell, Oxford, 1985, 312p.

13. Pillai, A. and Moorthy, P. Mineralogy and geochemistry of the red and black sediments of the Tuticorin district, Tamilnadu, India. Journal of Geological Society of Srilanka; 2014, 15: 47-56.

14. Nesbitt, H.W. and Young, G.M. Early Proterozoic climates of sandstone mudstone suites using SiO2 content and K2O/Na2O ratio. Nature; 299; 1982. p. 715-717.

15. McLennan SM, Hemming S, McDaniel DK, Hanson GN, Geochemical approaches to sedimentation, provenance, and tectonics, in Johnson M.J. Basu A. editors. Processes Controlling the Composition of Clastic Sediments: Geological Society of America, Special Paper; 284; 1993. p. 40-21.

16. Cullers, R.L, Implications of elemental concentrations for provenance, redox conditions, and metamorphic studies of shales and limestones near Pueblo, CO, USA. Chemical Geology.191 (4); 2002. p. 327-305.

17. Hayashi K, Fujisawa H, Holland H, Ohmoto H, Geochemistry of ~1.9 Ga sedimentary rocks from northeastern Labrador, Canada. Geochimica et Cosmochimica Acta; 61(19); 1997. p. 4137-4115.

18. Floyd PA, Winchester JA, Park RG, Geochemistry and tectonic setting of Lewisianclasticmeta sediments from the Early Proterozoic Loch Maree Group of Gairloch, N.W. Scotland. Precambrian Research; 45(1-3); 1989. p. 214-203.

19. Floyd PA, Leveridge BE, Tectonic environment of the Devonian Gramscatho Basin, south Cornwall: framework mode and geochemical evidence from turbiditic sandstones. Journal of the Geological Society. 144 (4); 1987. p. 542-531.

20. Cook E, Trueman C, Taphonomy and geochemistry of a vertebrate microremains assemblage from the Early Triassic karst deposits at Czatkowice 1, southern Poland. Palaeontologia Polonica; 65: 2009. p. 30-17.

21. Green MG, Sylvester PJ, Buick R, Growth and recycling of early Archean continental crust: geochemical evidence from the Coonterunah and Warrawoona Groups, Pilbara Craton, Australia. Tectonophysics; 322; 2000. p. 88-69.

22. Hallberg RO, A geochemical method for investigation of palaeoredox conditions in sediments. Ambio, Special Report; 4; 1976. p. 147-139.

23. Jones B, Manning DC, Comparison of geochemical indices used for the interpretation of paleo-redox conditions in Ancient mudstones. Chemical Geology; 111(1-4); 1994. p. 129-111.

24. Nath BN, Bau M, Ramalingeswara RB, Rao CM, Trace and rare earth elemental variation in Arabian Sea sediments through a transect across the oxygen minimum zone. Geochimica et Cosmochimica Acta; 61(12); 1997. p. 2388-2375.

25. Nagarajan R, Madhavaraju J, Nagendra R, Armstrong-Altrin JS, Moutte J, Geochemistry of Neoproterozoicshales

of the Rabanpalli Formation, Bhima Basin, Northern Karnataka, southern India: implications for provenance and paleoredox conditions. Revista Mexicana de Ciencias Geológicas; 24(2); 2007. p. 160-150.

26. Harnois L, The CIW index: a new chemical index of weathering. Sediment. Geol. 55; 1988. p. 322-319.

27. Fedo CM, Nesbitt HW, Young, GM, Unraveling the effects of potassium metasomatism in sedimentary rocks and paleosols, with implications for paleoweathering conditions and provenance. Geology; 23; 1995. p. 924-921.

28. Cullers RL, The geochemistry of shales, siltstones, and sandstones of Pennsylvanian-Permian age, Colorado, USA: implication for provenance and metamorphic studies. Lithos; 51: 2000. p. 203-181.

29. Lerman A, Lakes: Chemistry, Geology, Physics. Geological Press, Beijing, 1989. p. 10-100 (in Chinese).

30. Suttner, L.J. and Dutta, P. K. Alluvial sandstone composition and paleoclimate. Framework mineralogy. Journal of Sedimentary Petrology; 1989, 56: 326-345.

31. Bhatia MR, Plate tectonics and geochemical composition of sandstones. Journal of Geology; 92: 1983. p. 193-181.

32. He J, Zhou Y, Li H, Study on geochemical characteristics and depositional environment of Pengcuolinchert, Southern Tibet. Journal of Geography and Geology; 3(1); 2011. p. 188-178.

33. Shaltami, O.R., Fares, F.F., EL Oshebi, F.M., Errishi, H. and Souza, R. (2018): Geochemistry of the terra rossa in the Al Jabal al Akhdar, NE Libya: Implications on provenance, paleoclimate, paleoweathering, paleooxygenation and tectonic setting. Geoinformatics 2018, Kiev, Ukraine, Proceeding Book; pp. 28-45.

34. Wood, D.A. (1980): The application of the Th-Hf-Ta diagram to problems of tectonomagmatic classification and establishing the nature of crustal contamination of Basaltic Lava of the British Tertiary Volcanic Province. Earth and Planetary Science; Letters: 50: 11-30.